

NUCLEAR DATA AND MEASUREMENTS SERIES

ANL/NDM-80

**Neutron Total Cross Section Measurements
in the Energy Region from 47 keV to 20 MeV**

by

W.P. Poenitz and J.F. Whalen

May 1983

**ARGONNE NATIONAL LABORATORY,
ARGONNE, ILLINOIS 60439, U.S.A.**

NUCLEAR DATA AND MEASUREMENTS SERIES

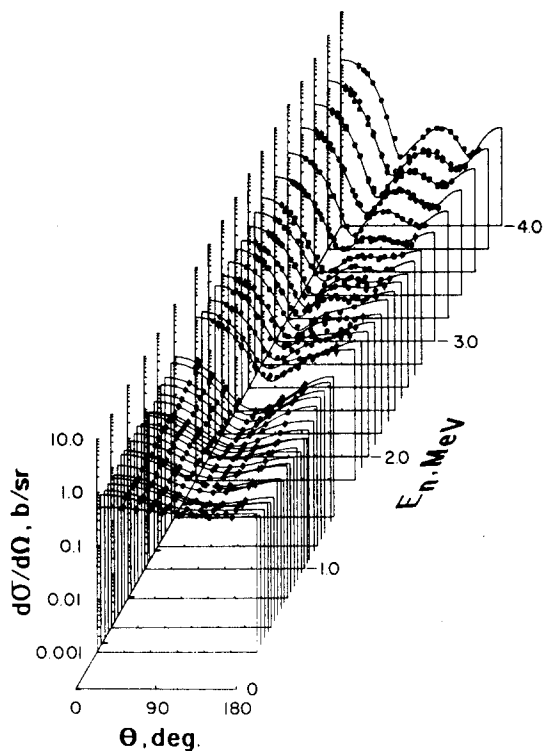
ANL/NDM-80

NEUTRON TOTAL CROSS SECTION MEASUREMENTS
IN THE ENERGY REGION FROM 47 keV to 20 MeV*

by

W. P. Poenitz and J. F. Whalen
Applied Physics Division

May, 1983



U of C-AUA-USDOE

ARGONNE NATIONAL LABORATORY,
ARGONNE, ILLINOIS 60439, U.S.A.

The facilities of Argonne National Laboratory are owned by the United States Government. Under the terms of a contract (W-31-109-Eng-38) among the U. S. Department of Energy, Argonne Universities Association and The University of Chicago, the University employs the staff and operates the Laboratory in accordance with policies and programs formulated, approved and reviewed by the Association.

MEMBERS OF ARGONNE UNIVERSITIES ASSOCIATION

The University of Arizona	The University of Kansas	The Ohio State University
Carnegie-Mellon University	Kansas State University	Ohio University
Case Western Reserve University	Loyola University of Chicago	The Pennsylvania State University
The University of Chicago	Marquette University	Purdue University
University of Cincinnati	The University of Michigan	Saint Louis University
Illinois Institute of Technology	Michigan State University	Southern Illinois University
University of Illinois	University of Minnesota	The University of Texas at Austin
Indiana University	University of Missouri	Washington University
The University of Iowa	Northwestern University	Wayne State University
Iowa State University	University of Notre Dame	The University of Wisconsin-Madison

NOTICE

This report was prepared as an account of work sponsored by the United States Government. Neither the United States nor the United States Department of Energy, nor any of their employees, nor any of their contractors, subcontractors, or their employees, makes any warranty, express or implied, or assumes any legal liability or responsibility for the accuracy, completeness or usefulness of any information, apparatus, product or process disclosed, or represents that its use would not infringe privately-owned rights. Mention of commercial products, their manufacturers, or their suppliers in this publication does not imply or connote approval or disapproval of the product by Argonne National Laboratory or the U. S. Department of Energy.

ANL/NDM-80

NEUTRON TOTAL CROSS SECTION MEASUREMENTS
IN THE ENERGY REGION FROM 47 keV to 20 MeV*

by

W. P. Poenitz and J. F. Whalen
Applied Physics Division

May, 1983

*This work supported by the U.S. Department of Energy

Argonne National Laboratory
9700 South Cass Avenue
Argonne, Illinois 60439
USA

NUCLEAR DATA AND MEASUREMENTS SERIES

The Nuclear Data and Measurements Series presents results of studies in the field of microscopic nuclear data. The primary objective is the dissemination of information in the comprehensive form required for nuclear technology applications. This Series is devoted to: a) measured microscopic nuclear parameters, b) experimental techniques and facilities employed in measurements, c) the analysis, correlation and interpretation of nuclear data, and d) the evaluation of nuclear data. Contributions to this Series are reviewed to assure technical competence and, unless otherwise stated, the contents can be formally referenced. This Series does not supplant formal journal publication but it does provide the more extensive information required for technological applications (e.g., tabulated numerical data) in a timely manner.

INFORMATION ABOUT OTHER ISSUES IN THE ANL/NDM SERIES:

A list of titles and authors for reports ANL/NDM-1 through ANL/NDM-50 can be obtained by referring to any report of this series numbered ANL/NDM-51 through ANL/NDM-70. Requests for a complete list of titles or for copies of previous reports should be directed to:

Section Secretary
Applied Nuclear Physics Section
Applied Physics Division
Building 316
Argonne National Laboratory
9700 South Cass Avenue
Argonne, Illinois 60439
USA

- ANL/NDM-51 Measured and Evaluated Neutron Cross Sections of Elemental Bismuth by A. Smith, P. Guenther, D. Smith and J. Whalen, April 1980.
- ANL/NDM-52 Neutron Total and Scattering Cross Sections of ${}^6\text{Li}$ in the Few MeV Region by P. Guenther, A. Smith and J. Whalen, February 1980.
- ANL/NDM-53 Neutron Source Investigations in Support of the Cross Section Program at the Argonne Fast-Neutron Generator by James W. Meadows and Donald L. Smith, May 1980.
- ANL/NDM-54 The Nonelastic-Scattering Cross Sections of Elemental Nickel by A. B. Smith, P. T. Guenther and J. F. Whalen, June 1980.
- ANL/NDM-55 Thermal Neutron Calibration of a Tritium Extraction Facility using the ${}^6\text{Li}(n,t){}^4\text{He}/{}^{197}\text{Au}(n,\gamma){}^{198}\text{Au}$ Cross Section Ratio for Standardization by M. M. Bretscher and D. L. Smith, August 1980.
- ANL/NDM-56 Fast-Neutron Interactions with ${}^{182}\text{W}$, ${}^{184}\text{W}$ and ${}^{186}\text{W}$ by P. T. Guenther, A. B. Smith and J. F. Whalen, December 1980.
- ANL/NDM-57 The Total, Elastic- and Inelastic-Scattering Fast-Neutron Cross Sections of Natural Chromium, Peter T. Guenther, Alan B. Smith and James F. Whalen, January 1981.
- ANL/NDM-58 Review of Measurement Techniques for the Neutron Capture Process by W. P. Poenitz, August 1981.
- ANL/NDM-59 Review of the Importance of the Neutron Capture Process in Fission Reactors, Wolfgang P. Poenitz, July 1981.
- ANL/NDM-60 Neutron Capture Activation Cross Sections of ${}^{94}\text{Zr}$, ${}^{96}\text{Zr}$, ${}^{98,100}\text{Mo}$, and ${}^{110,114,116}\text{Cd}$ at Thermal and 30 keV Energy, John M. Wyrick and Wolfgang P. Poenitz, (to be published).

- ANL/NDM-61 Fast-neutron Total and Scattering Cross Sections of ^{58}Ni by Carl Budtz-Jørgensen, Peter T. Guenther, Alan B. Smith and James F. Whalen, September 1981.
- ANL/NDM-62 Covariance Matrices and Applications to the Field of Nuclear Data, by Donald L. Smith, November 1981.
- ANL/NDM-63 On Neutron Inelastic-Scattering Cross Sections of ^{232}Th , ^{233}U , ^{235}U , ^{238}U , ^{239}U , and ^{239}Pu and ^{240}Pu by Alan B. Smith and Peter T. Guenther, January 1982.
- ANL/NDM-64 The Fission Fragment Angular Distributions and Total Kinetic Energies for $^{235}\text{U}(n,f)$ from 0.18 to 8.83 MeV by James W. Meadows, and Carl Budtz-Jørgensen, January 1982.
- ANL/NDM-65 Note on the Elastic Scattering of Several MeV Neutrons from Elemental Calcium by Alan B. Smith and Peter T. Guenther, March 1982.
- ANL/NDM-66 Fast-neutron Scattering Cross Sections of Elemental Silver by Alan B. Smith and Peter T. Guenther, May 1982.
- ANL/NDM-67 Non-evaluation Applications for Covariance Matrices by Donald L. Smith, July 1982.
- ANL/NDM-68 Fast-neutron Total and Scattering Cross Sections of ^{103}Rh by Alan B. Smith, Peter T. Guenther and James F. Whalen, July 1982.
- ANL/NDM-69 Fast-neutron Scattering Cross Sections of Elemental Zirconium by Alan B. Smith and Peter T. Guenther, December 1982.
- ANL/NDM-70 Fast-neutron Total and Scattering Cross Sections of Niobium by Alan B. Smith, Peter T. Guenther and James F. Whalen, July 1982.
- ANL/NDM-71 Fast-neutron Total and Scattering Cross Sections of Elemental Palladium by Alan B. Smith, Peter T. Guenther and James F. Whalen, June 1982.
- ANL/NDM-72 Fast-neutron Scattering from Elemental Cadmium by Alan B. Smith and Peter T. Guenther, July 1982.
- ANL/NDM-73 Fast-neutron Elastic-Scattering Cross Sections of Elemental Tin by C. Budtz-Jørgensen, Peter T. Guenther and Alan B. Smith, July 1982.
- ANL/NDM-74 Evaluation of the ^{238}U Neutron Total Cross Section by Wolfgang Poenitz, Alan B. Smith and Robert Howerton, December 1982.

- ANL/NDM-75 Neutron Total and Scattering Cross Sections of Elemental Antimony by Alan B. Smith, Peter T. Guenther and James F. Whalen, November 1982.
- ANL/NDM-76 Scattering of Fast-Neutrons from Elemental Molybdenum by Alan B. Smith and Peter T. Guenther, November 1982.
- ANL/NDM-77 A Least-Squares Method for Deriving Reaction Differential Cross Section Information from Measurements Performed in Diverse Neutron Fields by Donald L. Smith, November 1982.
- ANL/NDM-78 Fast-Neutron Total and Elastic-Scattering Cross Sections of Elemental Indium by A. B. Smith, P. T. Guenther, and J. F. Whalen, November 1982.
- ANL/NDM-79 Few-MeV Neutrons Incident on Yttrium C. Budtz-Jørgensen, P. Guenther, A. Smith and J. Whalen, September 1982.

Table of Contents

	<u>Page</u>
Abstract	1
I. Introduction	2
II. Experimental Methods and Techniques	3
II.1. Basic Method	3
II.2. Neutron Sources, Energy Scales, and the Experimental Setup	4
II.3. The Samples and the Sample Changer	8
II.4. Neutron Detectors, Dead Time Determination, and Data Acquisition	9
III. Measurements and Corrections.	11
III.1. Measurements.	11
III.2. Corrections	12
IV. Results and Discussions	13
References	27

NEUTRON TOTAL CROSS SECTION MEASUREMENTS
IN THE ENERGY REGION FROM 47 keV to 20 MeV*

by

W. P. Poenitz and J. F. Whalen

Applied Physics Division
Argonne National Laboratory

ABSTRACT

Neutron total cross sections were measured for 26 elements. Data were obtained in the energy range from 47 keV to 20 MeV for 11 elements in the range of light-mass fission products. Previously reported measurements for eight heavy and actinide isotopes were extended to 20 MeV. Data were also obtained for Cu (47 keV to 1.4 MeV) and for Sc, Zn, Nd, Hf, and Pt (1.8 to 20 MeV). The present work is part of a continuing effort to provide accurate neutron total cross sections for evaluations and for optical-model parameterizations. The latter are required for the derivation of other nuclear-data information of importance to applied programs.

*This work was supported by the U.S. Department of Energy.

I. Introduction

Fast-neutron total cross sections have been measured for more than three decades. The first systematic investigation over wide mass and energy regions, by Barschall et al. (1), not only refuted prior theoretical predictions (2), but, more importantly, helped in the derivation of the optical model (OM, e.g., Ref. 3), which remains of substantial importance to this day. A large fraction of the existing data information for fission-product nuclei and higher actinides has been derived from (or with the help of) optical/statistical-model calculations. Such calculations depend on parameter sets which in turn have been obtained by fitting available experimental values. Consequently, the accuracy of a large amount of data presently used in the applied area depends not only on the uncertainties and limitations of the nuclear-model descriptions, but also on the quality of the available experimental-data base. The neutron total cross sections play an important role in such OM descriptions as they are the quantities which can be calculated with the least ambiguities.

The transport cross section used in reactor-neutronics calculations depends on the neutron total cross section, σ_t , but reactor parameters are not very sensitive to the neutron total cross section (4). This is the consequence of low neutron leakage from power reactors and from most critical test assemblies. However, smaller critical facilities, like GODIVA and JEZEBEL, are appreciably more sensitive to σ_t , due to their higher neutron leakage.

The need for accurate neutron total cross sections is evident in other instances. An important recent application involved the derivation of the total neutron-inelastic-scattering cross sections of the actinides as the difference between the total cross section and the elastic-scattering cross section as well as other partial cross sections (5). This example is a turnabout from the common practice in evaluations of determining the elastic-scattering cross section as the difference between the total cross section and other partial cross sections. Another recurrent need for accurate total cross sections is for the calculation of corrections for transmission and scattering effects in experiments made for the determination of other cross sections. The neutron total cross section, of course, remains of key importance for evaluations since the other partial cross sections must add up to it.

Although this is not a complete list of applications, it shows that accurate neutron total cross sections are often required. In view of this need, it is surprising that an inspection of the available data base (for example in BNL-325 (6)) indicates substantial discrepancies for many nuclei, and a complete lack of data in some energy regions for others. This is even more astonishing since the measurement of a neutron total cross section is considered one of the simpler tasks in a neutron laboratory. Despite this situation, CINDA (7) indicates that very few new data have been reported in the last 10-15 years.

The goal of the present program is to provide accurate energy-averaged neutron total cross section data for use in optical-model assisted evaluations. The emphasis so far has been on heavy nuclei, specifically the actinides

Th-232, U-233, U-235, U-238, Pu-239, and Pu-240, and on the isotopes and elements in the light-mass range of the fission-products. The interest in the actinide region was due to their direct use in the applied area and due to their use in the determination of OM parameters, required for the fitting of neutron-capture cross sections (8) and the calculation of neutron-inelastic-scattering cross sections (9,10). The need for neutron total cross sections in the range of the light-mass fission products arose again due to their use in the determination of OM parameters (11), and also due to their use in the calculation of neutron scattering and transmission corrections for capture cross section measurements (11,12). The energy range was chosen to coincide with essentially the entire energy range of energy-average cross sections in evaluated data files (e.g., ENDF/B-V (13)) and to provide sufficient overlap with the unresolved-resonance range. At the same time, this energy region covers the range over which the neutron total cross sections of most nuclei display prominent maxima or minima, each due to the OM-described features of nuclear interactions.

Because the measured cross sections vary only slowly with energy, the energy-grid density at which measurements were carried out was not considered important beyond the objective of obtaining a good description of the OM gross structure. White-spectra neutron source time-of-flight measurements follow their own law in this regard, however, for most of the monoenergetic measurements, the energy-grid density of the values was chosen not to be linear but rather closer to an equal-lethargy basis (though not explicitly so). The extension of the measurements to low neutron energies (~ 500 keV) was considered an essential feature of the present experiments because the neutron-capture cross sections are important for the applied area in this range, and capture-cross-section calculations with the statistical model are sensitive to optical model parameters (11). The use of an OM parameter set which does not describe the neutron total cross section well in this region would surely be unsatisfactory.

Some of the data for heavy and actinide nuclei for energies up to 4.5 MeV have been published (14,15). For these, the present report describes the extension of the measurements to higher energies (20 MeV). For the range of light-mass fission products, the data presented here cover the entire energy range from 47 keV to 20 MeV. The experimental technique has been previously summarized, and it will be described in detail here because of the later extensions of the measurements and in order to provide a complete and accurate account for later reference and analysis.

II. Experimental Methods and Techniques

II.1. Basic Method

Neutron cross section data will be useful in future evaluations if the data, the experiment, the data reduction, the corrections and the estimated uncertainties are properly reported. However, their usefulness depends as well on the experimental design. Even if the data reporting was complete and

the description of the experiment sufficient, reevaluation of a data set by application of corrections which were recognized to be required at a later time, or by updating of corrections with improved secondary data or calculational procedures, will not increase the weight of a data set with inherently poor experimental design relative to others.

The best experimental design for a planned measurement is one in which all uncertainties are minimized based on present state-of-the-art techniques and methodological procedures. This should be the aim of the experimenter, however, the best possible design may be in conflict with cost-and-time considerations so that a compromise has to be found. Such compromises must be carefully considered since a measurement which provides data of poorer quality than those already available would be pointless.

The neutron total cross sections were obtained in the present experiment with the transmission (16) and the neutron time-of-flight (TOF) techniques. The identified components of such measurement which might be improved upon by experimental design are:

1. Neutron-source monitors.
2. Neutron detectors.
3. Suppression of background.
4. Control of dead-time effects.
5. Elimination of in-scattering effects.
6. Application and verification of resonance self-shielding corrections.
7. Sample-parameter optimization.

The neutron-source monitors were eliminated in the present experiments. State-of-the-art neutron detectors for the present type of measurements were used. Background effects were controlled by time-of-flight measurements with monoenergetic neutrons, the use of shadowbars, and the application of pulse-shape discrimination. In-scattering effects were made negligible by choosing an appropriate geometry for the set-up. Dead-time effects were controlled by the introduction of a time-correlated random pulser. The last two items on the above list were affected by the aforementioned need for compromise. Shelf-shielding effects can be investigated by measuring the transmission as a function of the sample thickness, and minimum statistical uncertainty can be obtained in the energy range where shelf-shielding is negligible by optimizing the sample size (16). However, both these approaches require extensive (and expensive) sample sets as well as substantially extended measuring times. Thus, the present measurements were carried out with samples which were already available, and corrections for self-shielding effects were calculated. The latter calculations were experimentally checked for some of the elements at selected energies. The various effects and corrections will be discussed in subsequent sections where appropriate.

II.2. Neutron Sources, Energy Scales, and the Experimental Set-up

Measurements were carried out with a variety of different neutron sources. A thick lithium target and the ${}^7\text{Li}(p,n)$ reaction were used as a

source with a pseudo-white neutron-energy spectrum up to 200 keV. In the intermediate-energy range (0.2 - 4.5 MeV) "monoenergetic" neutrons were obtained with the ${}^7\text{Li}(p,n)$ reaction and target thicknesses corresponding to 20 - 80-keV-neutron-energy spreads. Finally, measurements at higher neutron energies were made with the ${}^7\text{Li}(d,n)$ reaction using thick lithium targets as a source to provide a pseudo-white spectrum up to ~ 20 MeV.

The primary proton or deuteron beams, pulsed and bunched to approximate 1 nsec., were obtained from an 8-MV Tandem-Dynamitron accelerator. The repetition rates which were varied according to the energy range and measurement set are given in Table I.

At low neutron energies, the energy scale was determined with well-known resonances of iron (17) by using a 4-cm-long elemental-iron cylinder as one of the samples. In the intermediate-energy range, the digital-voltmeter reading from a resistor string attached to the high-voltage terminal of the accelerator was calibrated with resonances of Si (0.566 MeV, Ref. (18)) and C (2.078 MeV, Refs. (18, 19, 20)), the cross-section minimum of C at 3.01 MeV (18), and the thresholds of the ${}^7\text{Li}(p,n)$ and ${}^{10}\text{B}(p,n)$ reactions. The neutron-energy spreads were determined from the widths of the measured resonances and these were used to obtain the thickness of the target. The latter was then used together with the energy loss of protons in lithium to determine the neutron-energy spread for the specific energies at which cross section values were measured.

The energy scale for the higher neutron-energy measurements was determined by averaging the transmission through carbon as derived with ENDF/B-V cross section values (21) and matching the present data to it. The latter was necessary due to the short flight path of 8 m and the uncertainty of the time-zero position in the spectra.

The experimental set-up is shown schematically in Fig. 1. The total flight paths varied from set to set and they are given in Table 1. For data set 4, the neutron detector was a 2-cm-thick, 12.7-cm-diameter-NE213

TABLE I. Summary of Experimental Data Sets

Data Set	Neutron Source	Energy Range MeV	Flight Path, m	Repetition Rate, MHz	Detector
1	${}^7\text{Li}(p,n)$, white ^a	0.03 - 0.23	3.32	0.5	BND-S ^c
2	${}^7\text{Li}(p,n)$, mono ^b	0.22 - 1.6	3.32	2	BND-S
3	${}^7\text{Li}(d,n)$, white ^e	1.8 - 20.0	8.414	1	BND-M, PSD ^d
4	${}^7\text{Li}(p,n)$, mono ^b	0.98 - 4.5	7.909	2	NE213, PSD
14	${}^7\text{Li}(p,n)$, white ^{a,f}	0.079	3.74	1	BND-S
	mono ^{b,f}	0.5, 1.0	3.74	2	BND-S
	mono ^{b,g}	0.36 - 1.4	3.74	2	BND-S

^aWhite neutron spectrum with maximum energy of ≈ 0.23 MeV.

^b"Monoenergetic" neutrons, 20-80 keV width.

^cDetector radius 5 cm, height 15 cm.

^dDetector radius 7.62 cm, height 17.78 cm.

^eWhite neutron spectrum with maximum energy of ≈ 23 MeV.

^fOnly for In, Sn, Mo, Zr, Nb, Y.

^gOnly for Zr.

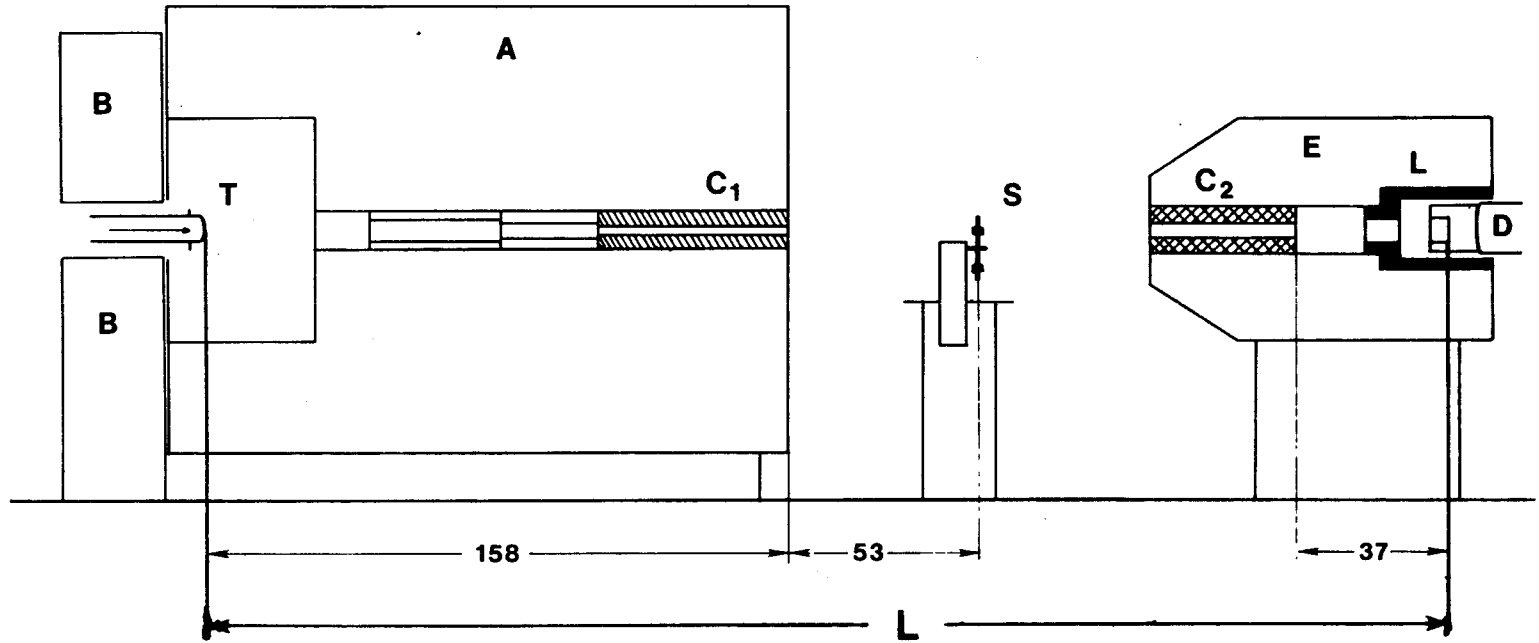


Fig. 1. Schematic of the Experimental Set-up. The total flight paths, L , are given in Table 1. T is the neutron source, S indicates the samples and the sample changer, and D shows the neutron detector. A and B are neutron-source shields, E and L are detector shields. The collimator C1 limits the number of neutrons which strike the samples, and the collimator C2 defines the primary neutron beam.

scintillator without the detector shield shown in the figure. Inscattering effects (which are determined by the space angle with which the samples are illuminated, the space angle of the primary and of the secondary scattered neutrons, and the forward-versus-isotropic scattering ratio) were negligible with the given distances between the neutron source and the samples, and between the samples and the neutron detectors.

II.3. The Samples and the Sample Changer

The thicknesses of the samples used in the various measurement sets are given in units of atoms per barn in Table 2. Also listed are the densities of these samples (in g/cm^3) and the corresponding values from reference tables for comparison (22).

In some cases, additional unspecified uncertainties exist due to the requirement of enclosing certain samples in stainless steel cans. This concerns the Nd sample which was canned many years ago, and an inspection and remeasurement of the sample dimensions was not possible at this time. Some of the actinide samples (U-233, Pu-239, and Pu-240) were canned several years ago after careful measurements of their dimensions and weights had been made. However, it is known that the natural alpha decay of these nuclei results in physical deformations. Again, it was not feasible to remeasure the dimensions. The neutron total cross section of Te was measured in the present experiments, but it was found to be grossly discrepant with data by others with whom our results for other elements agree to within approximately 1% or better. This was attributed to uncertainties of the sample which had been canned many years ago. Therefore, the resulting data have not been included in the present report.

As mentioned in Section II.1., an improvement of the basic measurement method was possible with the elimination of the neutron-source monitors. This was achieved using specific features of the sample changer. First attempts were made with a continuously rotating sample wheel (23), and a sample wheel driven with an electromagnetic stepping motor (24). Finally, in order to improve the efficiency and the reliability of the operation, a sample wheel driven by a cam-index mechanism was used to move an eight-position sample wheel in a rapid stepping motion. The wheel can be rotated with variable speed, but in the present measurements a maximum of 0.28 RPS was used. Thus, the measured spectra were accumulations of short-time (approximately 310 ms) data acquisition periods. Fluctuations of the neutron-source intensity for the sample and void spectra were averaged, and the need for a neutron-source monitor was eliminated.

The wheel had 8 notches equally spaced around the perimeter which triggered a photodiode. The photodiode signals were used to advance a 3-bit counter which identified the samples. An additional notch on the wheel and a photodiode were used to reset this counter after each revolution of the wheel. A second wheel on the gear rotated with constant speed four times per revolution of the sample wheel and had a variable notch. A photodiode on this second wheel was used to trigger a precision univibrator which provided the gate signal for

accepting detector counts during the time the sample area overlapped completely with the neutron beam area. Due to the highly non-linear angular velocity of the sample wheel, the sample moves very slowly as it approaches and leaves the static position. This allows an appreciable amount of time for counting while the sample is totally within the neutron beam but still moving. By varying the notch position on the second wheel and corresponding extension of the gate pulse, a portion of the time the sample is still moving can be included. A maximum efficiency of approximately 80% for samples with a diameter of 2.54 cm could be achieved. However, because of the variable sizes of the samples used in the present experiments, the gate was triggered only when the samples were at rest and the gate width adjusted such that it closed when the samples started to move. This resulted in an efficiency of approximately 67%. Since only one open position was required for 7 samples, the overall efficiency was higher than in a conventional sample-in-sample-out experiment. The correct operation of the system was tested with a random detector signal which yielded agreement between the accepted signals for each sample position within 0.05%.

II.4. Neutron Detectors, Dead-Time Determination, and Data Acquisition

For low neutron energies, extending up to 1.6 MeV, a "small" Black Neutron Detector (BND, Ref. 25) was used. This type of detector has a high efficiency even at low neutron energies and provides a low sensitivity to gain shifts of the photomultiplier. Later development (26) led to the application of pulse-shape discrimination to such relatively large-size scintillation detectors, and one of these BND's was used in the white-spectrum high-energy measurements (1.8 MeV - 20 MeV). A NE-213-scintillation detector with pulse-shape discrimination was used for some of the monoenergetic measurements in the medium-energy range. The detector types and their sizes are given in Table 1.

A timing signal was obtained with a constant-fraction discriminator from the fast anode pulses of the neutron-detector photomultiplier. This signal was mixed with a time-correlated random pulser signal in an OR-gate and then used to start a time-to-amplitude converter. The purpose of the time-correlated random pulser was to determine dead-time perturbations of the measurements. It was derived from a fast coincidence between a random pulse, extended in length to about the spacing of two accelerator beam pulses, and the accelerator beam pulse. This procedure results in peaks in the time-of-flight spectra which clearly define losses due to dead-time effects of the entire system (electronics as well as from computer data acquisition hard and software origins). The procedure was tested by measuring with polystyrene (CH) samples of various thicknesses, resulting in different dead-time corrections. Agreement was found for the effective cross sections of CH within the statistical accuracy of the test (approximately 0.1 - 0.2%).

Subsequent data acquisition and partial data processing was done with an on-line computer system (27). Modifications were made such that in most cases final cross section results could be obtained at any time during the measurements. This provided verification of correct equipment operation and experimental-progress control.

Table 2. Sample Specifications

Sample	Atms/Barn	Density g/cm ³	Density:	Ref. Set	1	2	3	4	14
Sc	0.0804	2.995	2.992				X		
Cu(2)	0.0420	8.849	8.96						X
Cu(3)	0.0837	8.842	8.96						X
Cu(1+7)	0.2386	8.911	8.96						X
Cu(5)	0.3338	8.808	8.96						X
Cu(6)	0.1597	8.845	8.96						X
Cu(4+8)	0.4901	8.883	8.96						X
Zn	0.1334	7.105	7.133				X		
Y	0.0597	4.405	4.45		X	X		X	
Y(1-4)	0.1175	4.488	4.45						X
Y(5)	0.0293	4.488	4.45						X
Y(1)	0.0617	4.476	4.45				X		
Zr(1)	0.1649	6.503	6.53				X		X
Zr(2)	0.0646	6.484	6.53		X	X		X	X
Nb(A)	0.0673	8.573	8.57						X
Nb(B+C)	0.1414	8.588	8.57						X
Nb(D+E+F)	0.2121	8.582	8.57						X
Nb(E+F)	0.1414	8.587	8.57				X		
Nb	0.0960	7.453	8.57		X	X			
Mo(1)	0.2552	10.228	10.22				X		X
Mo(2)	0.0642	10.188	10.22						X
Mo	0.1595	10.144	10.22		X	X		X	
Rh	0.1479	12.425	12.41		X	X	X		
Pd	0.1376	11.977	12.02		X	X	X		
Ag(1)	0.1092	10.48	10.50		X	X		X	
Ag(2)	0.0702	10.363	10.50					X	
Cd	0.0730	8.606	8.65		X	X	X	X	
In(a)	0.0732	7.285	7.31						X
In(B+C)	0.1515	7.286	7.31						X
In	0.0768	7.238	7.31		X	X	X		
Sn(1)	0.0718	7.263	7.31		X	X			
Sn(2)	0.0940	7.277	7.31				X		
Sn(3)	0.0529	7.263	7.31					X	
Sb	0.0838	6.672	6.691		X	X	X		
Hf	0.0660	13.033	13.29				X		
Ta	0.1046	16.656	16.6				X		
Pt	0.0405	21.032	21.45				X		
Au	0.0846	19.221	19.32				X		
Th	0.0670	11.63	11.66				X		
Unat	0.0869	19.04	18.95				X		
U233	0.0944	17.72	18.64				X		
U235	0.0971	18.62	18.71				X		
Pu239	0.0892	19.45	19.84				X		
Pu240	0.0724	15.26	19.92				X		

III. Measurements and Corrections

III.1. Measurements

Neutron transmissions were measured in several experiments with overlapping energy regions. This provided for checks on appropriate background corrections and of the reproducibility achieved in the present experiments. The measurement sets are summarized in Table 1, and the data which are discussed in Section IV. and shown in Figs. 2-12 are identified with these sets numbers.

Set 1

This low-energy set was measured with a pseudo-white neutron spectrum. Although neutron detection with the BND is possible at energies as low as 10 keV, the need to obtain background ranges on both sides of the neutron time-of-flight spectrum, as well as time-range and count-rate considerations, required the use of a higher threshold. Data were obtained above 47 keV and up to 200 - 220 keV. Uncertainty limitations in this range are due to statistics and cross section values were obtained by averaging over larger energy intervals clearly defined by resonances of iron.

Set 2

Monoenergetic-neutron measurements with the BND and the same set-up as for set no. 1 were carried out between 200 keV and 1.6 MeV. The ${}^7\text{Li}(p,n)$ source reaction has a minimum yield in the 200-300 keV neutron energy range. Data obtained in this region have larger statistical uncertainties and tend to scatter somewhat more than expected based on the statistical uncertainties.

This data set overlaps with set no. 4 typically between 1.0 and 1.6 MeV. The data were repeatedly integrated in order to check the influence of different choices for background regions. No systematic effect was found.

Set 3

This set involved pseudo-white spectra measurements at higher neutron energies. A BND with pulse-shape discrimination was used. The low energy threshold was set such that background ranges were available at both sides of the neutron TOF spectra. A 64-cm-long plexiglas rod was mounted in one of the positions of the sample wheel. The corresponding spectrum was (after dead-time correction) subtracted from all other spectra. The residual background was subtracted by linear interpolation between ranges outside of the neutron TOF spectra.

The ${}^7\text{Li}(d,n)$ reaction with a thick target results in a structured spectrum with a minimum yield in the 8 - 10 MeV range. Background in this region was approximately 10%. Bias shifts of the amplifier and/or linear gate due to the high count rates in this measurement set were observed and found to be as

large as 0.05 channels (with approximately 1 nsec/ch). These shifts were corrected, however, they added to the uncertainty and might be the reason that the present data exhibit some scatter in the region of minimum neutron yield by amounts which exceed statistical uncertainties.

Set 4

This set involved monoenergetic-neutron measurements extending from 0.98 to 4.5 MeV. A NE-213-scintillation detector was used with pulse-shape discrimination which substantially reduced the background. Above 3.5 MeV, the selection of background ranges became more difficult because of the second neutron group of the ${}^7\text{Li}(p,n)$ reaction and an observed increase of the non-ambient background. As a consequence, data from this set scatter somewhat at the high-energy end of the measurement range relative to the results from set no. 3.

Set 14

This set includes measurements of some elements for which samples of different thicknesses were available. The main purpose was to verify the consistency between the values obtained from the extrapolation of the measured effective cross sections with the self-shielding-corrected cross sections.

III.2. Corrections

Corrections for in-scattering of neutrons were negligible due to the design of the experiment as discussed in Section II.2. Dead-time effects were corrected as discussed in Section II.3. Background subtraction (which might be considered a correction) was discussed in the previous Section III.1. Several other possible effects were considered (transmission through collimator walls, transmission through air instead of a sample-equivalent void), but they were found to be negligible.

The remaining major concern is the resonance-self-shielding effect, particularly at lower neutron energies. Corrections were applied based on Monte-Carlo simulations of the resonance structure as previously described (15). However, the medium-mass elements involved in the present measurements require additional comments:

Some of the elements (Pd, Cd, Sn) consist of a large number of isotopes with correspondingly reduced isotopic densities in the samples and small self-shielding effects. The cross sections of others (Y, Zr, Mo, Nb) show marked structure at the low energy end of the present measurements. The Monte-Carlo-calculated corrections are based upon average resonance parameters and spacings, thus one might suspect that these corrections are incorrect in local energy regions where the observed structure indicates fluctuations of the resonance parameters and/or spacings. However, if the data are used for optical model fits, it can be expected that correct average values for the OM parameters will be obtained.

Measurements were carried out for several materials (Y, Zr, Nb, Mo, In, Sn) with samples of different thicknesses. The cross sections obtained from the (linear) extrapolation of the measured effective cross sections were, in all cases, in good agreement with the values obtained for the corrected data measured with a specific sample thickness as specified in Table 2. These measurements were, in most cases, made at three different energies (see Table I.), however, for Zr which shows pronounced structure of the cross section at lower energies, measurements were carried out with two samples of different thicknesses over a larger energy range. The results obtained from the linear extrapolations of the effective cross sections agree well with the corrected cross section data and thus do not indicate the requirement of locally different corrections as suggested above. However, this still could be a serious problem for even lighter nuclei, and the data for Cu were only obtained from the extrapolation of the effective cross sections measured for samples of different thicknesses.

IV. Results and Discussions

The results from the present measurements are shown in Figs. 2-12. Corresponding values will be made available to the National Nuclear Data Center of Brookhaven National Laboratory. The uncertainties of the data are typically in the 1-3% range. At low energies (500 keV) a major contribution to the uncertainty comes from statistical uncertainties (derived from the counts for the sample as well as for the corresponding void, and appropriately propagated through the derivation of the cross section). Another larger contribution to the uncertainties at lower neutron energies is for the self-shielding correction (assumed as 30% of the correction). The statistical uncertainty of the dead-time correction was negligible for all measurements of sets 1, 2, 4, and 14, but causes a correlated-systematic uncertainty for set 3 which was typically 0.3 - 0.6%. Differences obtained for the cross sections derived from different choices of background subtraction were accounted for as systematic uncertainties and typically amount to 0.3%. Uncertainties due to the uncertainties of the sample thickness (at./b) were estimated from the densities of the samples and by comparison with the known densities for the element (see Section II.3.). Additional information was obtained for some elements from the comparison of different samples at 1 MeV neutron energy where resonance self-shielding was negligible. The contributions from sample uncertainties were typically 0.5-1.0%.

Carbon

The primary purpose for including carbon samples in most measurements, specifically in set 3, was to adjust the energy scale for the present measurements. However, it was recently suggested that the neutron total cross section of carbon of ENDF/B-V is too high by 8% in the energy region around 8 MeV (28). The present results are shown in Fig. 2 and compared with ENDF/B-V values. The ENDF/B-V values were averaged with a Gaussian resolution function. Small differences can be mainly justified by slight mismatches in the resolution functions. The present data agree well with the corresponding ENDF/B-V values, specifically in the energy region where the reduction of the cross sections by 8% has been proposed.

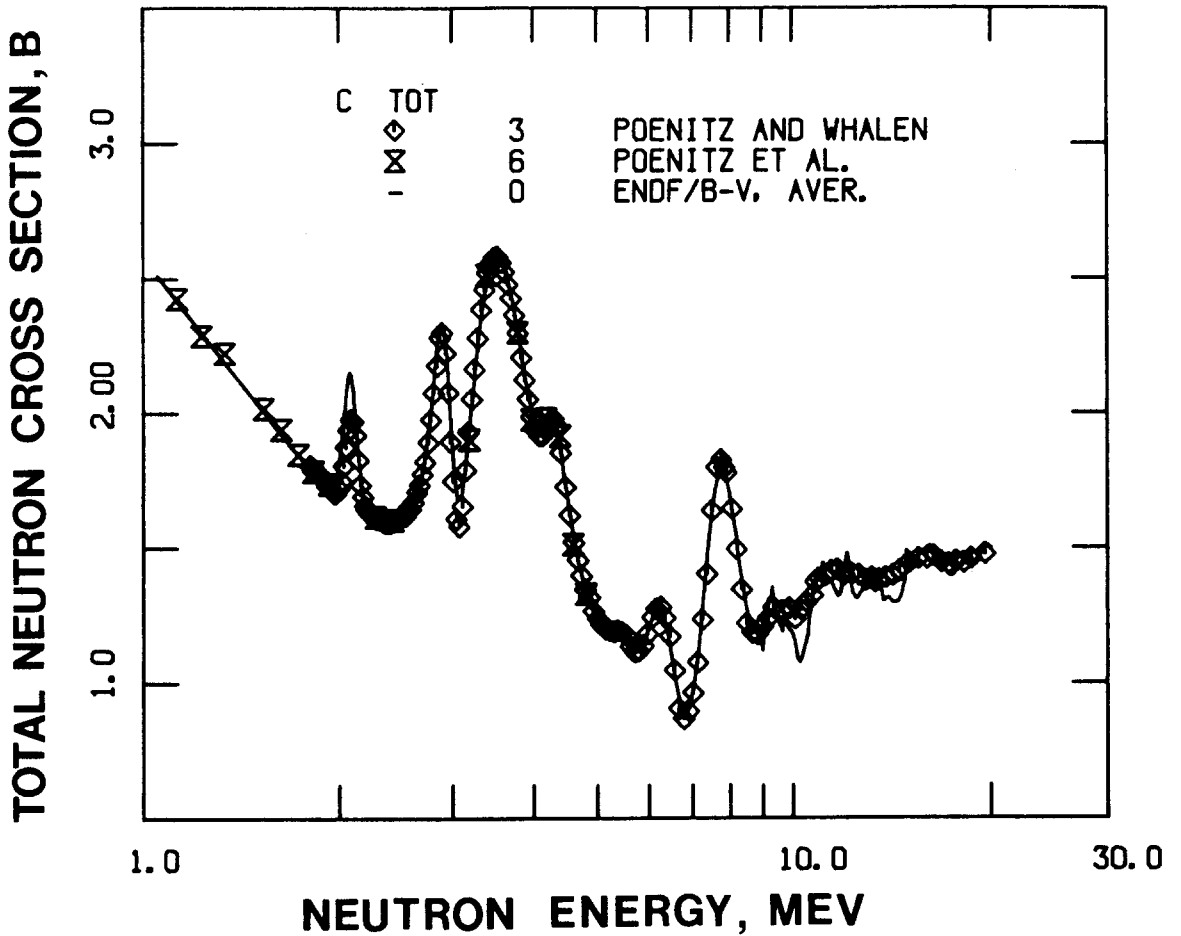


Fig. 2. The Present Results for the Neutron Total Cross Section of Carbon. Some previous data are also shown (15). The ENDF/B-V data up to 9 MeV have been averaged. Set numbers are defined in the text.

A somewhat curious point is the 2.078 MeV resonance. The present data appear not to match the area of this resonance as derived from ENDF/B-V cross sections. This also seems to be the case for other data sets used to derive the evaluated cross section (29).

Copper

Measurements were carried out for Cu only below 1.4 MeV. Data up to 4.5 MeV were recently measured with the same equipment and procedure (30). The present data are shown in Fig. 3 and were obtained from the (non-linear) extrapolations of the effective cross sections. These extrapolations were substantial over the sample thickness range from 0.04 at./b to 0.49 at./b (up to 60%) and large cross section fluctuations occur at low energies. Figure 4 shows the relative difference between the extrapolated cross sections and the effective cross sections averaged over 10 keV energy intervals obtained with a sample of 0.49 at./b. This demonstrates locally strongly fluctuating self-shielding effects, which are apparently much reduced for the heavier nuclides of Zr (as discussed above).

Scandium and Zinc

Data were obtained only in the 1.8 - 20-MeV-neutron-energy range and are shown in Fig. 5.

The Light-Mass Fission-Product Range - Y, Zr, Nb, Mo, Rh, Pd, Ag, Cd, In, Sn, and Sb

Data were measured over the entire energy range from 47 keV to 20 MeV. However, for Nb, Rh, Pd, In, Sn and Sb only two values were obtained between 1.0 and 1.8 MeV. Data are available for these elements from recent measurements made with essentially the same equipment and set-up (31-36). The present data are shown together with the latter in Figs. 6, 7, and 8.

Some Heavy-Mass Elements - Nd, Hf, Pt, Ta, and Au

Data were obtained only in the 1.8-20MeV energy range and are shown in Fig. 9 and 10. Data reported previously for Ta and Au (15) are shown in Fig. 10 for comparison.

The Actinides - Th, U-233, U-235, U, Pu-239, and Pu-240

The present measurements extend the range of previously reported data (14,15) to 20 MeV. The new measurements overlap with the previous values between 1.8 and 4.5 MeV. Both data sets are shown in Figs. 11 and 12. The corresponding values of the evaluated nuclear data file ENDF/B-V are also shown in these figures. The agreement between the present data and ENDF/B-V is only reasonably good for U-233 and U-238. It is fair for Th-232 and U-235, and poor for the two plutonium isotopes 239 and 240.

The present measurements provide neutron total cross section data over an extended energy range which are of importance for practical applications and for the derivation of optical model parameter sets. OM calculations and fits have not been carried out at this time. Such investigations should

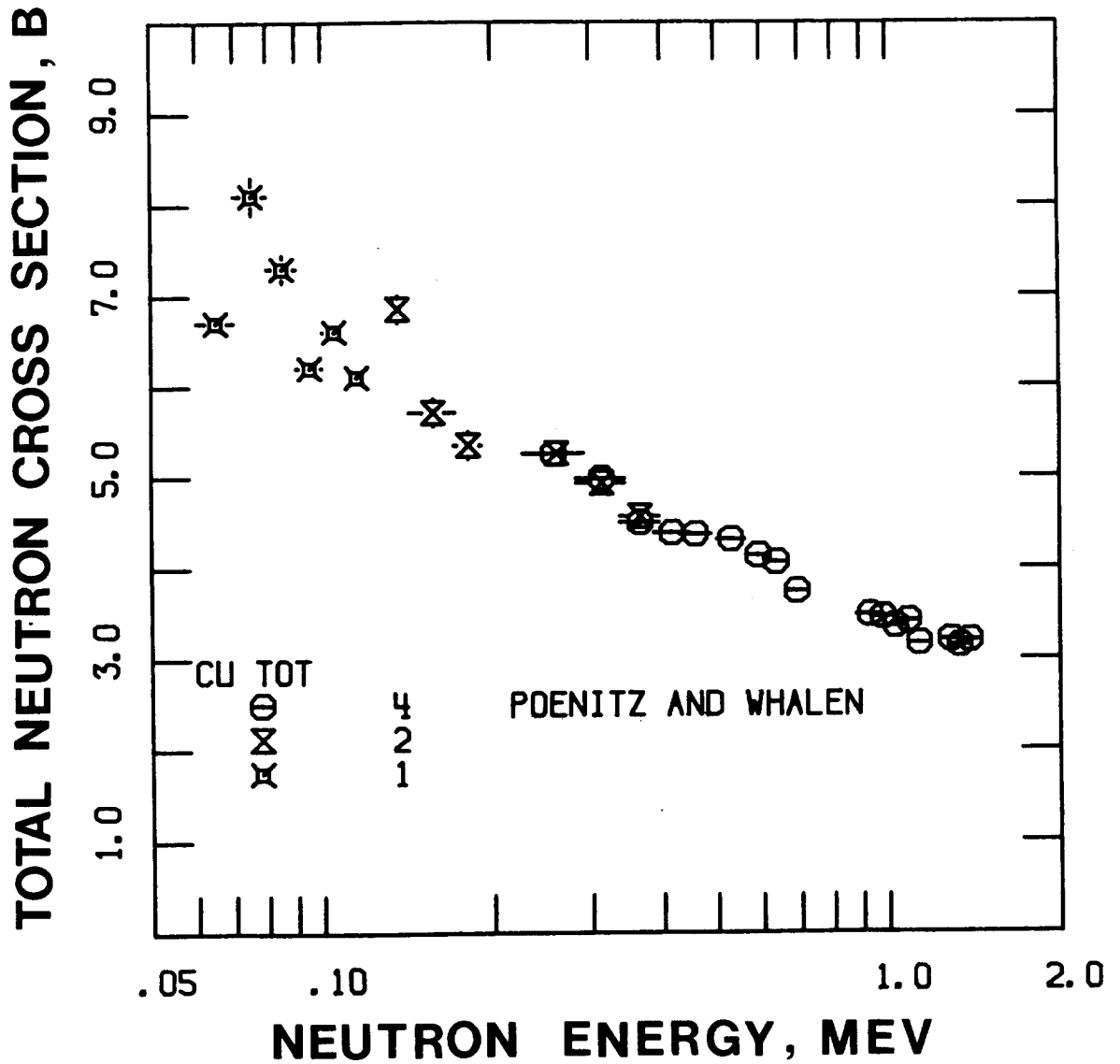


Fig. 3. The Present Results for the Neutron Total Cross Section of Elemental Copper. Set numbers are defined in the text.

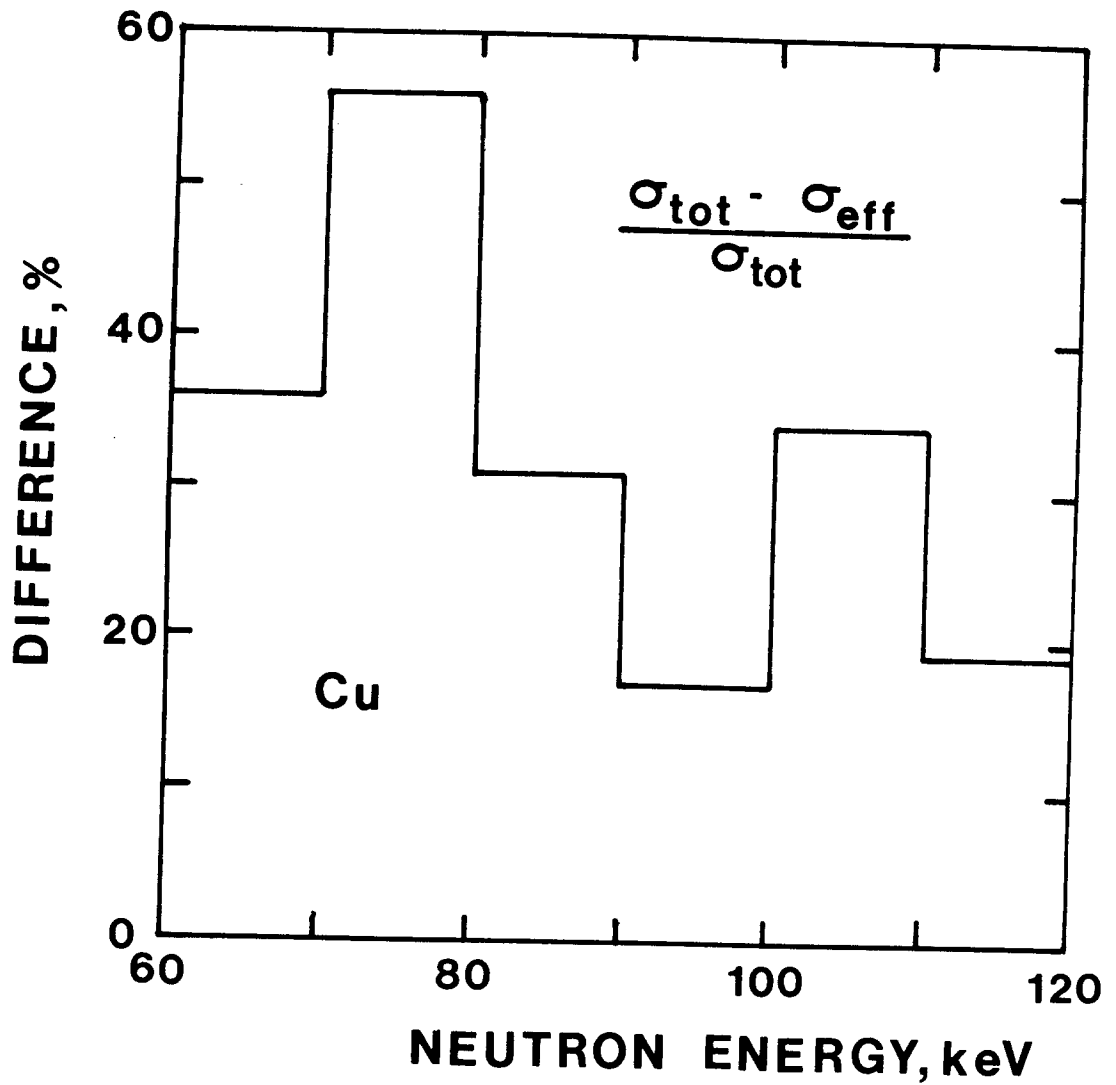


Fig. 4. The Relative Difference Between the Neutron Total Cross Section of Copper and the Effective Neutron Total Cross Section Measured for a 0.49 at./b Thick Sample.

be based on the best knowledge obtained from diverse experimental efforts, and thus require a careful examination of the complete available data base, e.g., an evaluation, as for example carried out for U-238 (37). Such evaluations are planned for the near future.

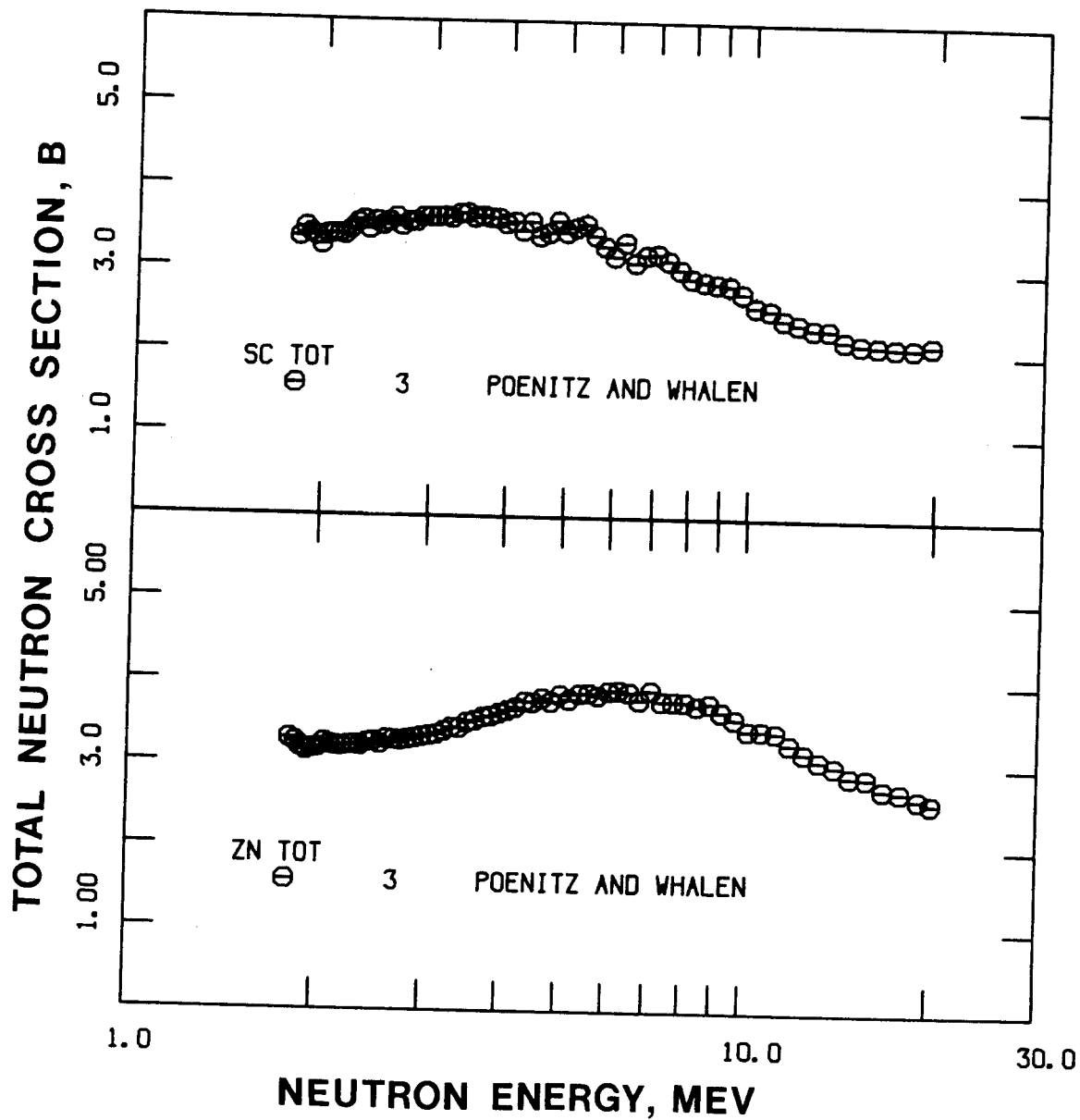


Fig. 5. The Present Results for the Neutron Total Cross Sections of Scandium and Zinc. Set numbers are defined in the text.

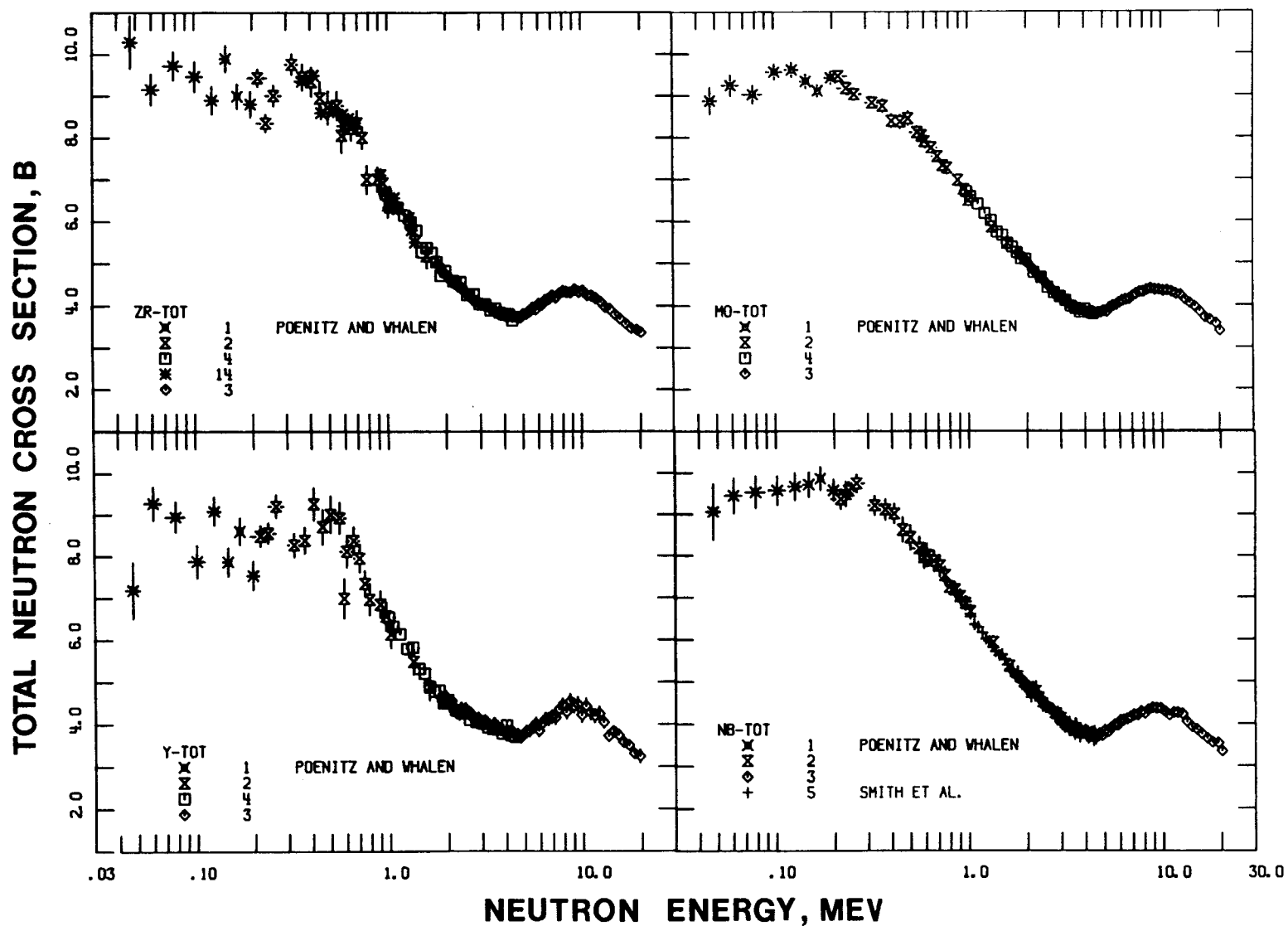


Fig. 6. The Present Results for the Neutron Total Cross Sections of Yttrium, Zirconium, Niobium, and Molybdenum. Recent measurements by Smith et al., (32) are shown for comparison. Set numbers are defined in the text.

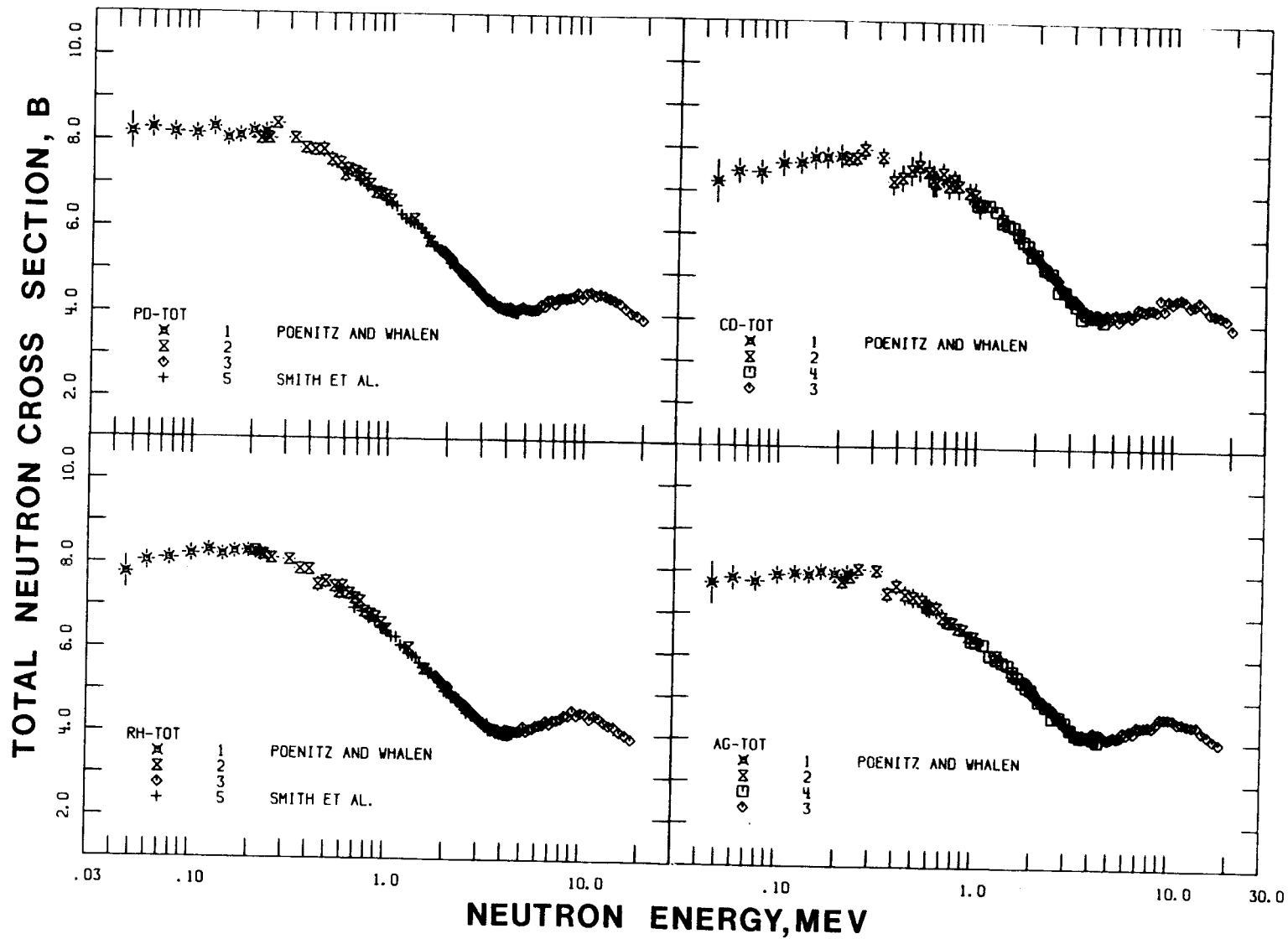


Fig. 7. The Present Results for the Neutron Total Cross Sections of Rhodium, Palladium, Silver, and Cadmium. Recent data by Smith et al., (31,33) are shown for comparison. Set numbers are defined in the text.

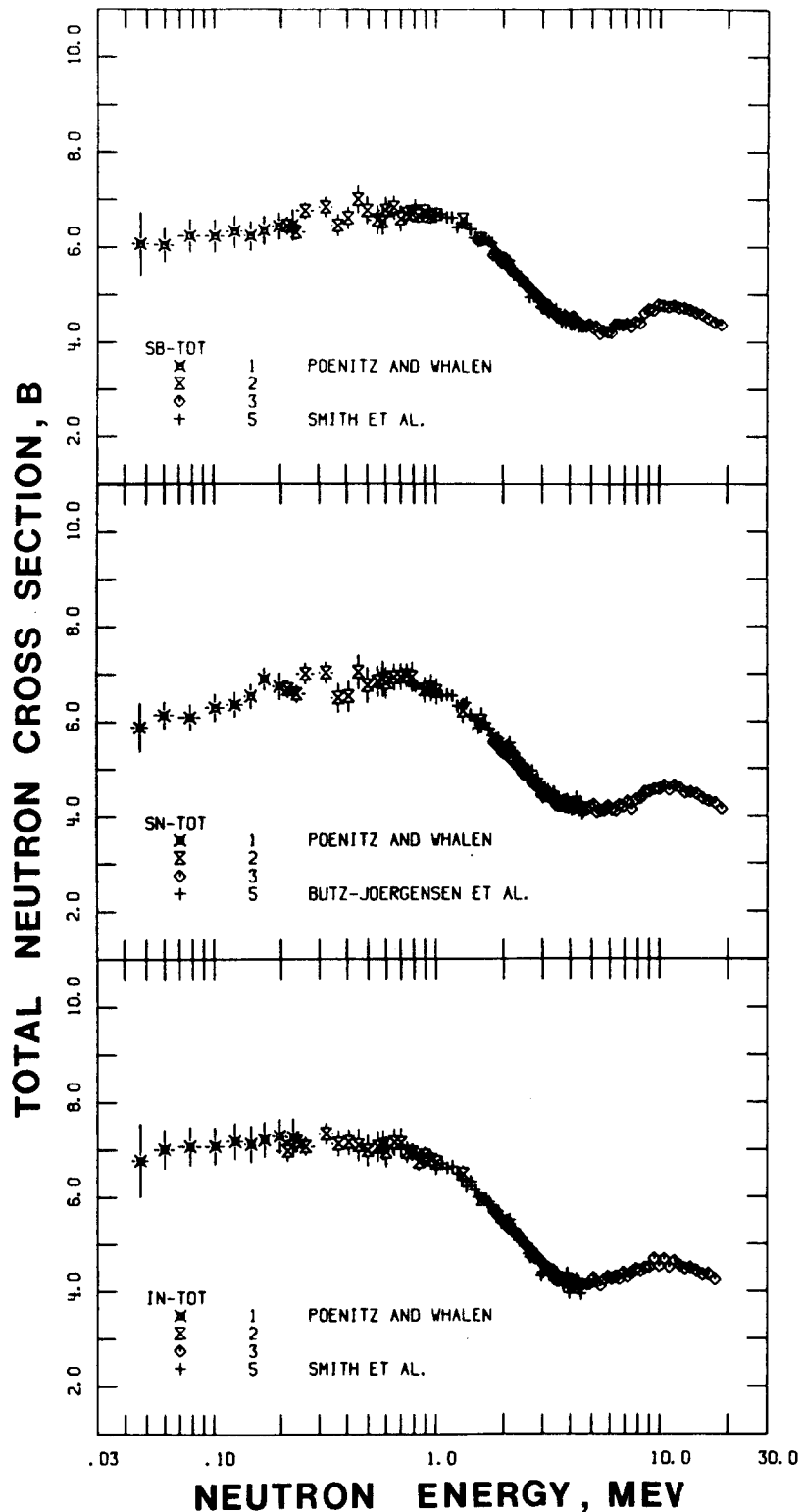


Fig. 8. The Present Results for the Neutron Total Cross Sections of Indium, Tin, and Antimony. Recent data by Smith et al., (35,36), and by Budtz-Jørgenson et al., (34) are shown for comparison. Set numbers are defined in the text.

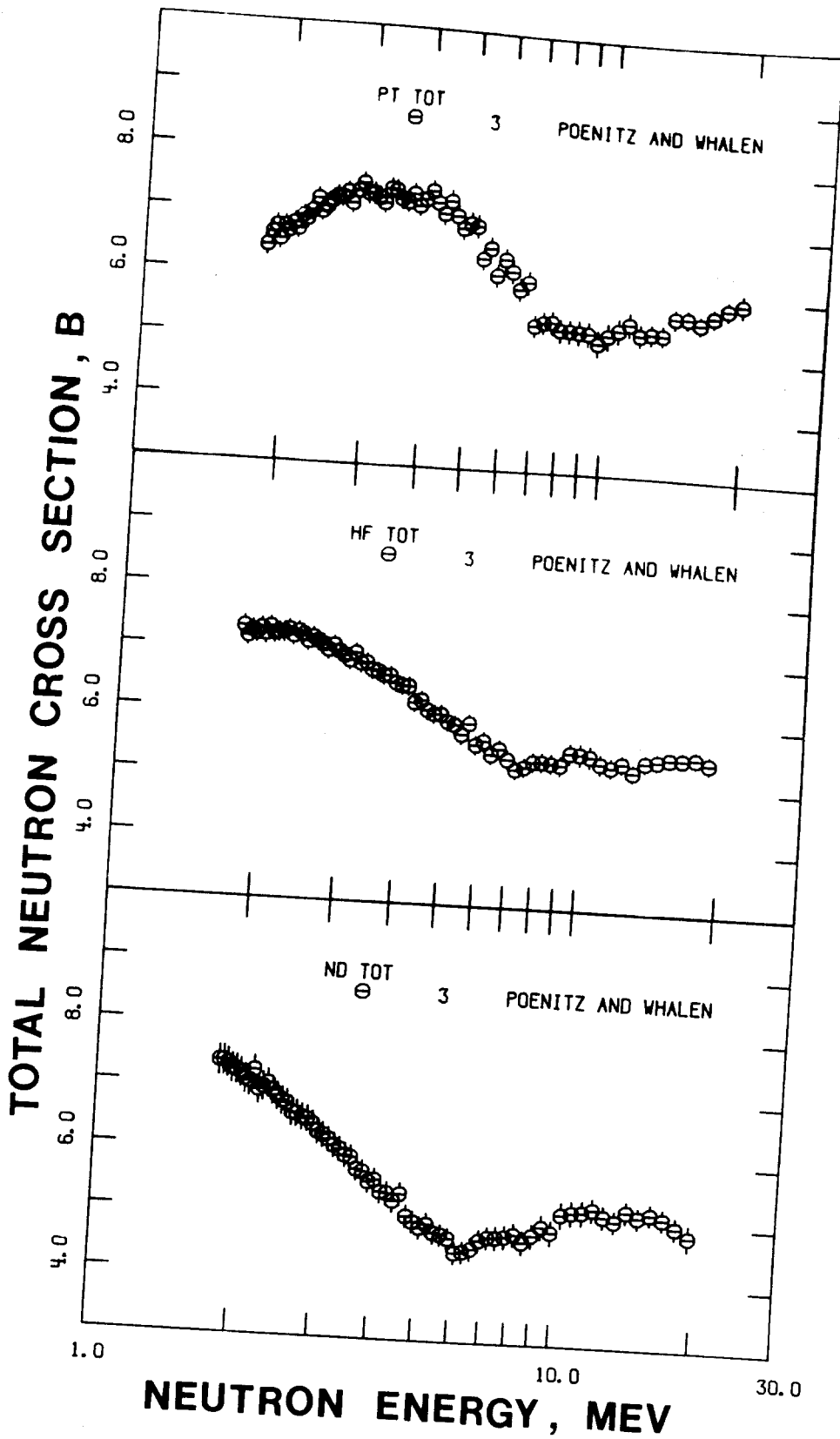


Fig. 9. The Present Results for the Neutron Total Cross Sections of Neodymium, Hafnium, and Platinum. Set numbers are defined in the text.

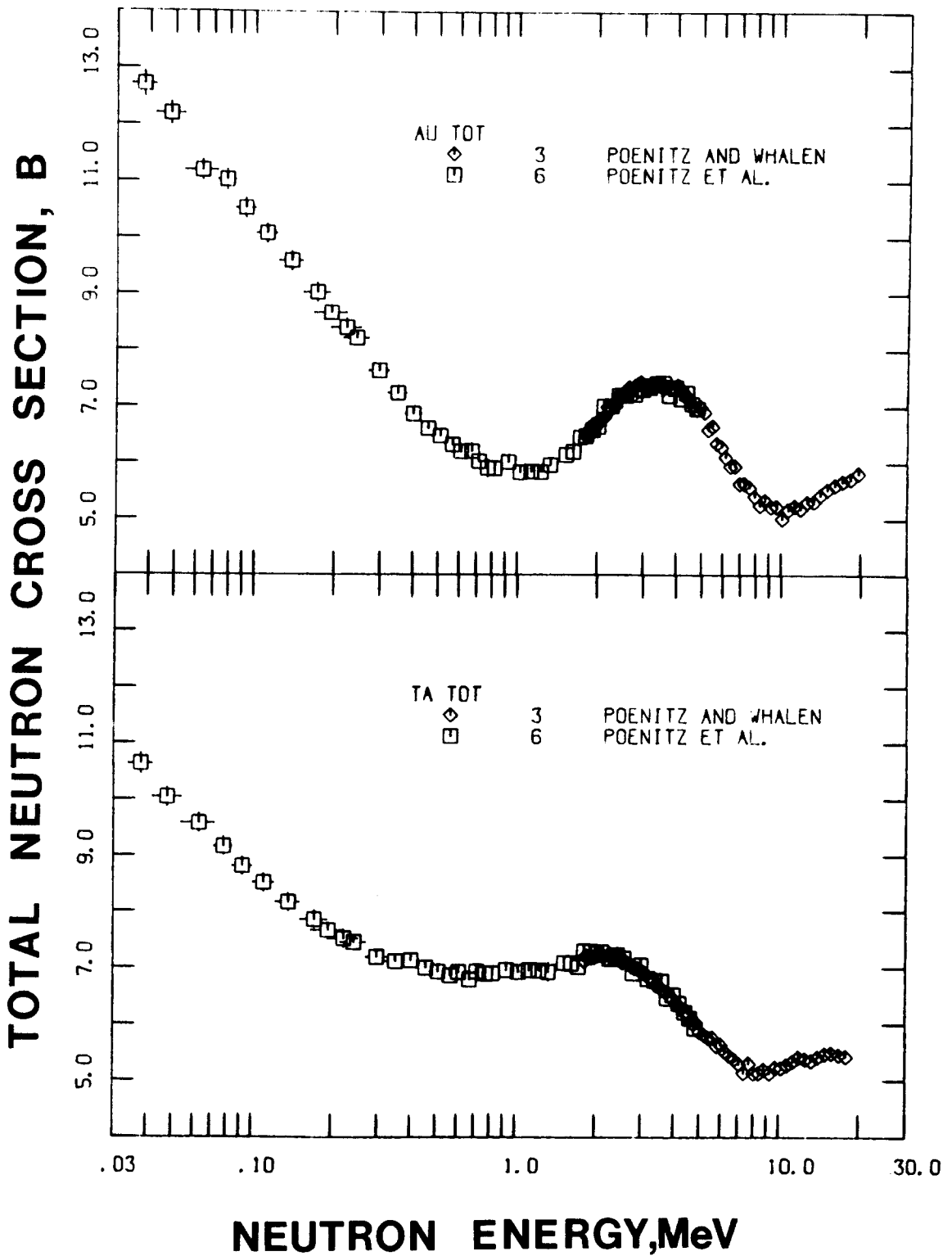


Fig. 10. The Present Results for the Neutron Total Cross Sections of Tantalum and Gold. Previously reported data (15) are shown for comparison. Set numbers are defined in the text.

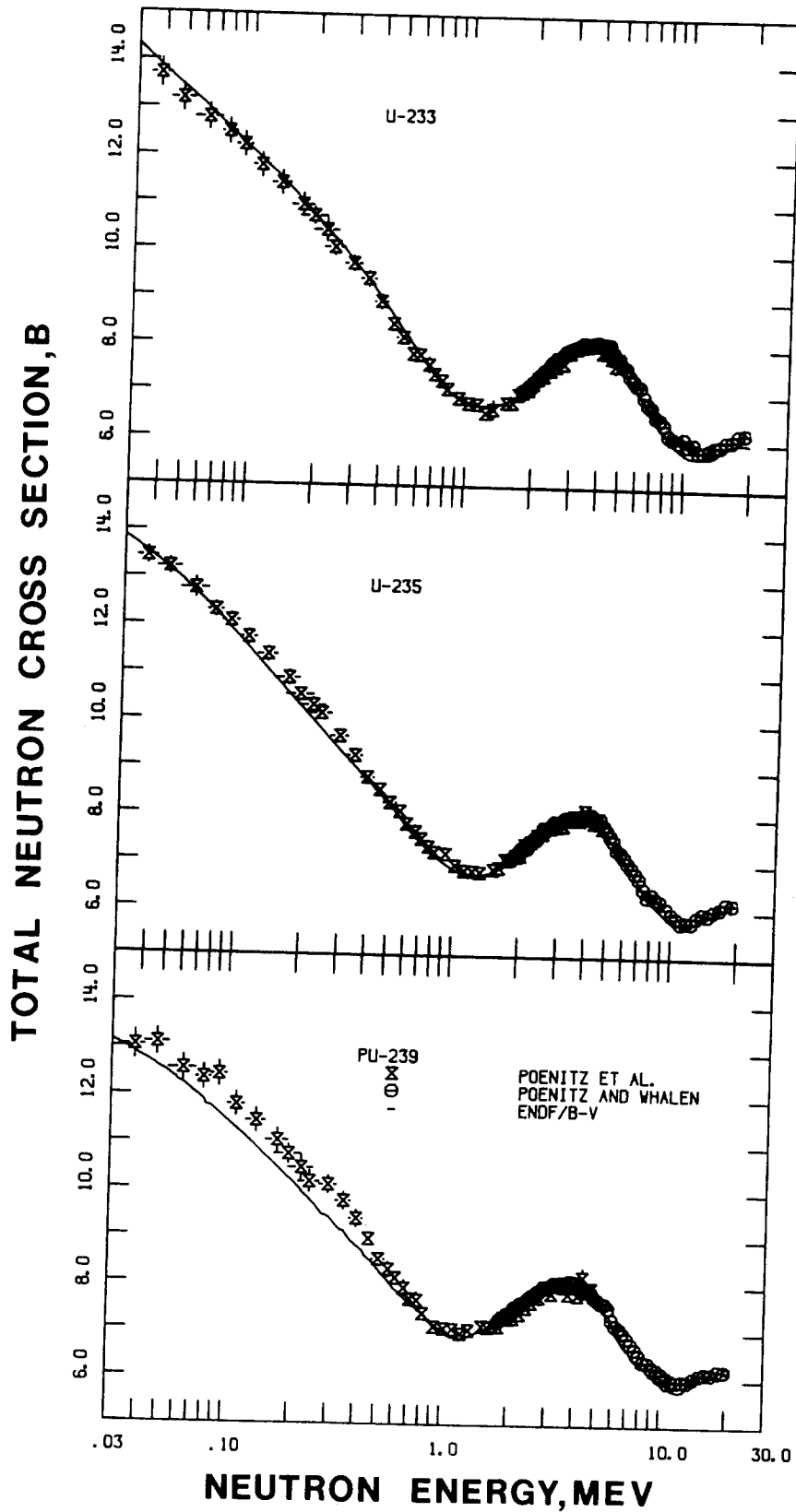


Fig. 11. The Present Results for the Neutron Total Cross Sections of the Fissile Nuclides U-233, U-235, and Pu-239. Previously reported data (15) and ENDF/B-V values are shown for comparison. Set numbers are defined in the text.

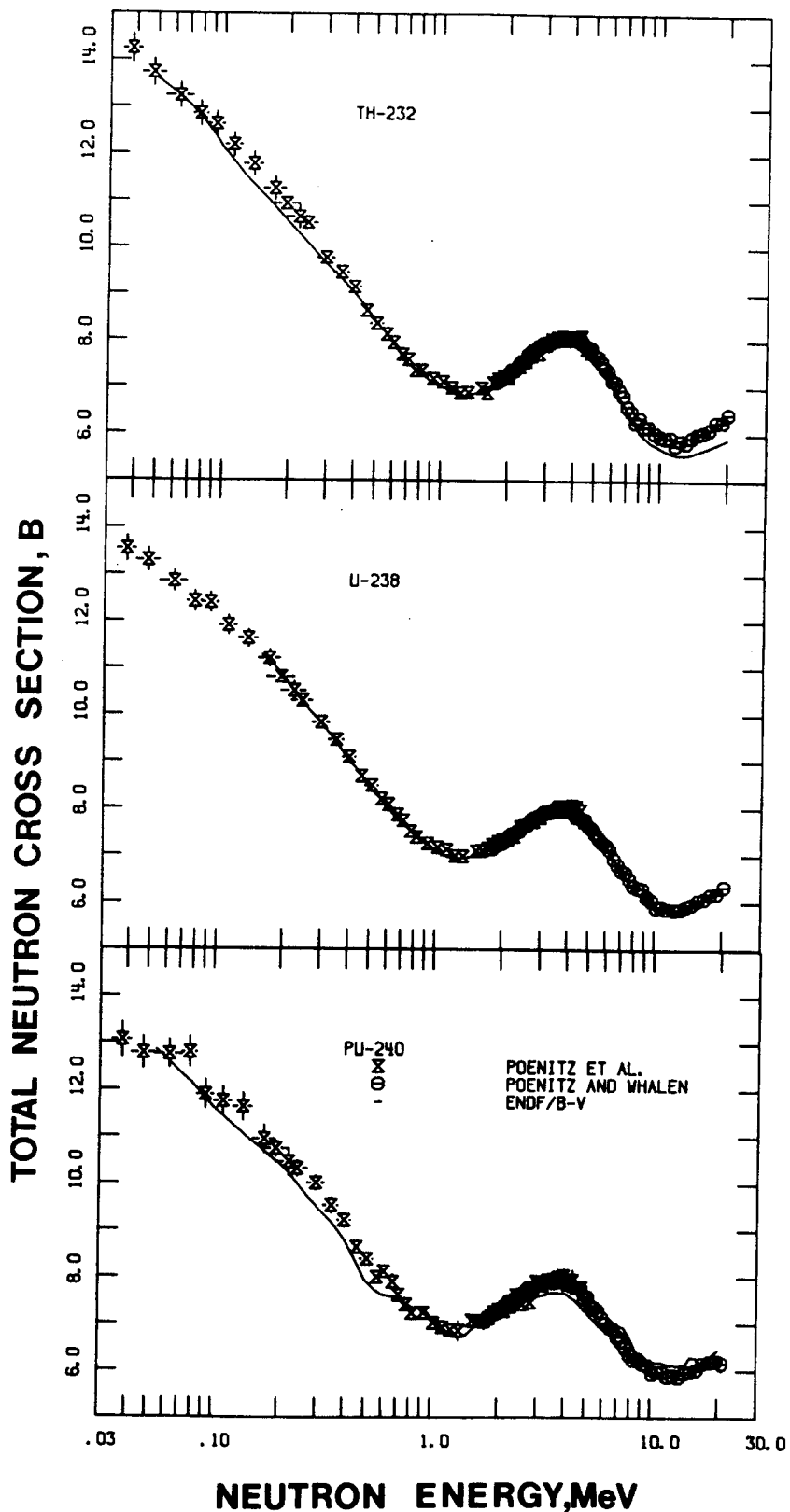


Fig. 12. The Present Results for the Neutron Total Cross Sections of the Fertile Nuclides Th-232, U-238, and Pu-240. Previously reported data (15) and ENDF/B-V values are shown for comparison. Set numbers are defined in the text.

References

1. H. Barschall, Phys. Rev. 86, 431 (1952); see also D. Miller et al., Phys. Rev. 85, 704 (1952), M. Walt and H. Barschall, Phys. Rev. 93, 1062 (1954).
2. H. Feshbach et al., Phys. Rev. 71, 145 (1947).
3. P. E. Hodgson, "The Optical Model of Elastic Scattering", Clarendon Press, Oxford (1963).
4. C. R. Weisbin et al., "Sensitivity Coefficient Compilation for CSEWG Data Test Benchmarks", ENDF-265, BNL-NCS-24853, Brookhaven National Laboratory (1978).
5. A. B. Smith et al., Proc. Conf. on Nuclear Data for Science and Technology, p. 39, Antwerp (1982).
6. D. I. Garber and R. R. Kinsey, "Neutron Cross Sections", Vol. II, BNL-325, Third Edition, Brookhaven National Laboratory (1976).
7. CINDA-A, also CINDA-82, "An Index to the Literature on Microscopic Neutron Data", International Atomic Energy Agency, Vienna (1979).
8. W. P. Poenitz, Proc. Conf. Nuclear Cross Sections for Technology, NBS Spec. Publ. 594, 368 (1979).
9. G. Antsipov et al., INDC(CCP)-116/CHJ, International Atomic Energy Agency (1981).
10. E. D. Arthur, Proc. Conf. On Nuclear Data for Science and Technology, p. 556, Antwerp (1982).
11. W. P. Poenitz, Proc. Spec. Meeting on Neutron Cross Sections of Fission Product Nuclei, p. 85, Bologna (1979).
12. W. P. Poenitz, Proc. Spec. Meeting on Fast Neutron Capture Cross Sections, ANL-83-4, 239, Argonne National Laboratory (1982).
13. ENDF/B, "Evaluated Nuclear Data File", R. Kinsey, Brookhaven National Laboratory.
14. W. P. Poenitz et al., Nucl. Sci. Eng. 68, 358 (1978).
15. W. P. Poenitz et al., Nucl. Sci. Eng. 78, 333 (1981).
16. D. Miller, in Fast Neutron Physics, Vol. II, Marion and Fowler, Edts., Interscience Publ., New York (1963).

References (Contd.)

17. ENDF/B-V, Fe, Mat No. 1326, C. Y. Fu and F. G. Perey, Eval., Oak Ridge National Laboratory (1977).
18. R. B. Schwarz et al., "MeV Total Neutron Cross Sections", NBS Monograph 138, National Bureau of Standards (1974).
19. G. D. James, Proc. Symp. on Neutron Standards for Applications, NBS Spec. Publ. 493, 319 (1977).
20. F. G. Perey, "Neutron Energy Standards", in ENDF-300, "Standard Reference and Other Important Nuclear Data; BNL-NCS-51123 (1979).
21. ENDF/B-V C, Mat. No. 1306, C. Y. Fu and F. G. Perey, Eval., Oak Ridge National Laboratory (1977), see also Ref. 29.
22. R. C. Weast et al., Handbook of Chemistry and Physics, The Chemical Rubber Co., Cleveland (1965).
23. J. F. Whalen, unpublished, Argonne National Laboratory (1971).
24. W. P. Poenitz, unpublished, Argonne National Laboratory (1971).
25. W. P. Poenitz, Nucl. Instr. Meth. 109, 413 (1973), also ANL-7915 (1972).
26. W. P. Poenitz and T. Tamura, Proc. Conf. on Nuclear Data for Science and Technology, p. 465, Antwerp (1982).
27. W. P. Poenitz and J. F. Whalen, "On-line Computer Facility and Operating System COSACS", ANL-8026, Argonne National Laboratory (1973).
28. R. W. Roussin et al., ENDF/B-V Shielding Data Testing Report, in ENDF-311, Brookhaven National Laboratory (1982).
29. C. Y. Fu and F. G. Perey, At. Data and Nucl. Data Tables 22, 249 (1978).
30. P. T. Guenther et al., BAPS 28, 4, HH4, 736 (1983).
31. A. B. Smith et al., "Fast Neutron Total and Scattering Cross Sections of Rh-103", ANL/NDM-68, Argonne National Laboratory (1982).
32. A. B. Smith et al., "Fast Neutron Total and Scattering Cross Sections of Niobium", ANL/NDM-70, Argonne National Laboratory (1982).
33. A. B. Smith et al., "Fast Neutron Total and Scattering Cross Sections of Elemental Palladium", ANL/NDM-71, Argonne National Laboratory (1982).
34. A. B. Smith et al., "Fast Neutron Total and Scattering Cross Sections of Elemental Tin", ANL/NDM-73, Argonne National Laboratory (1982).

References (Contd.)

35. A. B. Smith et al., "Fast Neutron Total and Scattering Cross Sections of Elemental Antimony", ANL/NDM-75, Argonne National Laboratory (1982).
36. A. B. Smith et al., "Fast Neutron Total and Scattering Cross Sections of Elemental Indium", ANL/NDM-78, Argonne National Laboratory (1982).
37. A. B. Smith et al., "Evaluation of the U-238 Neutron Total Cross Section", ANL/NDM-74, Argonne National Laboratory (1982).